CTP-TAMU-02-02

Detection of $B_s \to \mu^+\mu^-$ at the Tevatron Run II and Constraints on the SUSY Parameter Space

R. Arnowitt*, B. Dutta*, T. Kamon*,
M. Tanaka†

*Department of Physics, Texas A&M University, College Station TX 77843-4242,
†Argonne National Laboratory, Argonne, IL 60439.

(May 28, 2018)

Abstract

A measurement of the branching ratio for the rare decay mode $B_s \to \mu^+\mu^-$ at the Tevatron is an opportunity to test various supersymmetric scenarios. We investigate the prospects for studying this mode in Run II and estimate that CDF would be sensitive to this decay for a branching ratio $> 1.2 \times 10^{-8}$ with 15 fb^{-1}(or, if a similar analysis holds for D0, $> 6.5 \times 10^{-9}$ for the combined data). We calculate the branching ratio in minimal supergravity (mSUGRA) parameter space, and find that $\tan\beta > 30$ can be probed. (This mSUGRA parameter space cannot be probed by direct production of SUSY particles at Run II.) Including other experimental constraints on the mSUGRA parameter space, one finds that CDF $B_s \to \mu^+\mu^-$ measurements would be able to cover the full mSUGRA parameter space for $\tan\beta = 50$ if the muon $g_\mu - 2$ anomaly exceeds $\sim 11 \times 10^{-10}$, and about half the allowed parameter space for $\tan\beta = 40$. A large branching ratio $> 7(14) \times 10^{-8}$ (feasible with only 2 fb^{-1}) would be sufficient to exclude the mSUGRA model for $\tan\beta \leq 50(55)$. Dark matter neutralino-proton detection cross sections are examined in the allowed region, and should be large enough to be accessible to future planned experiments. Combined measurements of $B_s \to \mu^+\mu^-$, the Higgs mass m_h and the muon $g_\mu - 2$ anomaly would be sufficient to determine the $\mu > 0$ mSUGRA parameters (or show the model is inconsistent with the data). We also briefly discuss the $B_s \to \mu^+\mu^-$ decay in R parity violating models. There, for some models, the branching ratio can be large enough to be detected even for small $\tan\beta$ and large $m_{1/2}$.

1. INTRODUCTION. Supersymmetric (SUSY) extensions of the Standard Model (SM) represent a natural candidate for the new physics expected to occur in the TeV energy domain. One of the difficulties in determining predictions of such models lies in the large number of new parameters the theory implies. Thus the most general low energy model, the Minimal Supersymmetric Standard Model (MSSM), has over 100 free parameters, and even the minimal model based on supergravity grand unification at the scale $M_G = 2 \times 10^{16}$ GeV (mSUGRA) possesses four new parameters and one sign in addition to the SM parameters. Fortunately SUSY models apply to a large number of different accelerator and cosmological phenomena, and a great deal of effort has been involved in recent years to to use this data to limit the parameter space. Part of the difficulty in doing this resides in the success of the model in not disturbing the excellent agreement of the precision tests of the SM [1] due to the SUSY decoupling theorems which suppress SUSY contributions at low energies. Historically, the absence of flavor changing neutral currents at the tree level played an important role in the construction of the SM. They represent therefore an important class of phenomena that might show the presence of new physics, since the SM and the SUSY contributions contribute first at the loop level with comparable size. Thus the decay $b \to s\gamma$ has been a powerful tool in limiting the SUSY parameter space. In this paper, we consider the decay $B_s \to \mu^+\mu^-$ within the framework of mSUGRA models and R parity violating models. This process is particularly interesting for several reasons: The SM branching ratio is quite small, *i.e.*, $Br[B_s \to \mu^+\mu^-]_{\rm SM} = 3.5 \times 10^{-9}$ [2]. The SUSY contribution [3–8] has terms that grow as $\tan^6\beta$ (where $\tan\beta =< H_2 > / < H_1 >$ and $H_{1,2}$ are the two SUSY Higgs bosons) and thus can become quite large for large $\tan\beta$. Finally, as we shall show below, the two collider detectors at the Tevatron will be sensitive to this decay for $\tan\beta \gtrsim 30$ in Run II.

2. MSUGRA MODELS. We consider first mSUGRA models with R parity invariance, and combine the existing accelerator constraints on the parameter space (*e.g.*, the light Higgs mass m_h bound, $b \to s\gamma$ *etc.*), the cosmological dark matter constraints, the possible muon magnetic moment anomaly, with what might be expected from the Tevatron measurement of the $B_s \to \mu^+\mu^-$ decay. The combined constraints can significantly limit the SUSY parameter space, and thus allow better predictions as to what the models predict at the LHC.

The mSUGRA model [9,10] depends on four parameters which we take to be the following: m_0 (the universal scalar mass at M_G), $m_{1/2}$ (the universal gaugino mass at M_G), A_0 (the universal cubic soft breaking mass at M_G), and $\tan\beta$ (at the electroweak scale). In addition, the sign of μ (the Higgs mixing parameter appearing in the superpotential as $\mu H_1 H_2$) is arbitrary. We consider the parameter range of $m_0, m_{1/2} < 1$ TeV, $3 < \tan\beta < 55$, and $|A_0| < 4m_{1/2}$. We take a 2σ bound on the $b \to s\gamma$ decay [11] of $1.8 \times 10^{-4} < Br[b \to s\gamma] < 4.5 \times 10^{-4}$, and the LEP bound on the light Higgs of $m_h > 113.5$ GeV [12]. Since there is still a (2-3) GeV uncertainty in the theoretical calculation of m_h, we will (conservatively) interpret this to mean m_h(theory) > 111 GeV. For $\tan\beta \gtrsim 45$, results are sensitive to the precise values of m_b and m_t. We assume here that $m_b(m_b) = 4.25$ GeV and $m_t(pole) = 175$ GeV, and include the large $\tan\beta$ corrections to the b-quark Yukawa coupling constant [13]. We assume that any muon $g-2$ deviation from the SM is due to SUSY [14,15]. The experimental deviation has now been reduced to a $1.6\,\sigma$ effect [16,17], and we take here this deviation to be greater than 1σ below the current central value *i.e.*, $a_\mu^{\rm SUGRA} > 11 \times 10^{-10}$. We will show however, what would happen if this deviation were to change with the new BNL E821 data currently being analyzed. For mod-

els with R parity invariance, the lightest neutralino, $\tilde{\chi}_1^0$ is the dark matter particle, and we require that $0.07 < \Omega_{\tilde{\chi}_1^0} h^2 < 0.21$, in accord with current CMB and other astronomical data [18]. All stau-neutralino co-annihilation channels [19–21] are included in the relic density calculations.

3. $B_s \to \mu^+\mu^-$ DECAY. The branching ratio for $B_s \to \mu^+\mu^-$ is given in [5] which we write in the form

$$Br[B_s \to \mu^+\mu^-] = \frac{2\tau_B M_B^5}{64\pi} f_{B_s}^2 \sqrt{1-\frac{4m_l^2}{M_B^2}} \left[\left(1-\frac{4m_l^2}{M_B^2}\right)\left|\frac{(C_S-C_S')}{(m_b+m_s)}\right|^2 + \left|\frac{(C_P-C_P')}{(m_b+m_s)} + 2\frac{m_\mu}{M_{B_s}^2}(C_A-C_A')\right|^2\right] \quad (1)$$

where f_{B_s} is the B_s decay constant, M_B is the B meson mass, τ_B is the mean life and m_l is the mass of lepton. C_S, C_S', C_P, C_P' include the SUSY loop contributions due to diagrams involving the particles such as stop, chargino, sneutrino, Higgs etc.. For large $\tan\beta$, the amplitude has terms that grow like $\tan^3\beta$ as can be seen in the example of Figure 1. Thus at large $\tan\beta$, the dominant contribution to C_S is given approximately by

$$C_S \simeq \frac{G_F\alpha}{\sqrt{2}\pi} V_{tb}V_{ts}^* \left(\frac{\tan^3\beta}{4\sin^2\theta_W}\right)\left(\frac{m_b m_\mu m_t \mu}{M_W^2 M_A^2}\right)\frac{\sin 2\theta_{\tilde{t}}}{2}\left(\frac{m_{\tilde{t}_1}^2 \log\left[\frac{m_{\tilde{t}_1}^2}{\mu^2}\right]}{\mu^2-m_{\tilde{t}_1}^2} - \frac{m_{\tilde{t}_2}^2 \log\left[\frac{m_{\tilde{t}_2}^2}{\mu^2}\right]}{\mu^2-m_{\tilde{t}_2}^2}\right) \quad (2)$$

where $m_{\tilde{t}_{1,2}}$ are the two stop masses, and $\theta_{\tilde{t}}$ is the rotation angle to diagonalize the stop mass matrix. We need to muliply the above expression by $1/(1+\epsilon_b)^2$ to include the SUSY QCD corrections. ϵ_b is proportional to $\mu\tan\beta$ [22]. We have $C_P = -C_S, C_S' = (m_s/m_b)C_s$ and $C_P' = -(m_s/m_b)C_P$. The operators are given in ref. [5]. In our numerical calculation, we use all complete one loop contributions to the branching ratio.

4. DETECTION OF $B_s \to \mu^+\mu^-$ at TEVATRON. We consider now the possibility of detecting the decay $B_s \to \mu^+\mu^-$ by the CDF and D0 detectors at the Tevatron in Run II. Both detectors have been upgraded with excellent tracking and muon detector systems [2]. The dimuon trigger is the key to collect the $B_s \to \mu^+\mu^-$ decays.

In order to estimate the limits on $Br[B_s \to \mu^+\mu^-]$ detection, we use the 95% C.L. limit on $Br[B_s \to \mu^+\mu^-]$ published by CDF [23]. Thus our discussion is based on the CDF detector, although both CDF and D0 detectors should have a similar perfromance.

In the Run I analysis, CDF observed one candidate that was consistent with $B_s \to \mu^+\mu^-$ with an estimate of 0.9 backound (BG) events in 98 pb^{-1} [23]. The primary Run-I selection variables and cut values were that at least one muon track with $c\tau \equiv L_{xy}M_B/P_T^{\mu\mu} > 100\ \mu$m, $I \equiv P_T^{\mu\mu}/[P_T^{\mu\mu} + \Sigma P_T] > 0.75$ for the muon pair, and $\Delta\Phi < 0.1$ rad. Here, L_{xy} is the transverse decay length; $p_T^{\mu\mu}$ is the transverse momentum of the dimuon system. ΣP_T is the scalar sum of the transverse momenta of all tracks, excluding the muon candidates, within a cone of $\Delta R \equiv \sqrt{(\Delta\eta)^2+(\Delta\phi)^2} = 1$ around the monetum vector of the muon pair. The z coordinate of each track along the beam line [24] must be within 5 cm of the primary vertex. $\Delta\Phi$ is an opening azimuthal angle between $P_T^{\mu\mu}$ and the vector pointing from the primary vertex to the secondary vertex (the reconstructed B-meson decay position). As a

conservative estimate, CDF took the one event as signal to calculate 95% C.L. limit of signal events ($N_1^{95\%} \equiv$5.06 events [23]) and had set a limit of $Br < 2.6 \times 10^{-6}$. In the analysis, the selection efficiency (ϵ) for signal events and the rejection power ($\mathcal{R}$) for background events (pass a baseline selection [23]) are estimated to be $\epsilon_1 = 0.45$ and $\mathcal{R}_1 = 440$ by using a sample of like-sign dimuon events ($5 < M_{\mu\mu} < 6$ GeV/c^2).

A dimuon trigger in Ref. [2] will improve the acceptance for signal events by a factor of 2.8. The trigger will soon be tested using the Run IIa (2 fb^{-1}) data. This will allow us to modify the trigger design for the higher luminosity expected in Run IIb (15 fb^{-1}). In our analysis, we assume that the dimuon trigger can be designed by maintaing the acceptance for signal events. We expect to improve the acceptance for signal events by a factor of 2.8 [2]. If we assume the factor 2.8 to be the same for BG events, then we would observe 51 (386) events in 2 (15) fb^{-1} with the same cuts as in Run I. Therefore, CDF has to require a set of tighter cuts to obtain the best possible upper limit.

We first need to understand the background contents and expected improvement by the new Run II detector. Two types of backgrounds must be taken into account: (i) non-b backgrounds comming from the primary vertex; (ii) b background events, such as the gluon-spliting $b\overline{b}$ events.

The most important feature for B decays is the displaced vertex. One way to reduce prompt background is to require a minimum decay length L_{xy}. However, two tracks can appear to form a secondary vertex if one of two tracks originates from the primary vertex and the other has an impact parameter (d). Therefore, the requirement of a minimal impact parameter of individual tracks can further clean up the sample. It has been shown for example, in the Run-I analysis for $B^0 \to K^{0*}\mu^+\mu^-$ events [25], that a tight impact parameter cut on significance for individual track ($d/\sigma_d > 2$) significantly improve the background rejection even with $L_{xy} > 100$ μm. One has then $\epsilon \sim \epsilon_1 \times 0.43$ and $\mathcal{R} \sim \mathcal{R}_1 \times 190$.

We indeed observed the similar numbers of OS and LS events in the Run-I final selection for $B_s \to \mu^+\mu^-$ events, while we should expect more OS events than LS events if the cuts were tight enough for non-b background events. This indicates the final dimuon event candidates in Run I analysis are actually dominated by the non-b background sources. Thus a higher track impact parameter is neccessary to reduce the non-b backgrounds. We would expect larger reduction with good efficiency even after the L_{xy} cut. In other words, we would have been able to set better limits if we had included the impact parameter for the cut optimization. The silicon vertex detector (SVX-II) will provide us much better reduction for the non-b background than Run I. The non-b background will not be a problem in Run II.

In Run II, the most severe background will be the two muons from gluon-spliting $b\overline{b}$ events. Since both particles are b quarks, the impact parameter does not help. Both b and $\overline{b}$ also go in the same direction, so that cut on L_{xy} does not help either. However, $\Delta\Phi$ is still usefull to remove the background events. Furthermore, in Run II, we can use $\Delta\Theta$ in r-z view since we have z-strips in SVX-II.

There is some room to improve the isolation cut. We can form a new isolation parameter by only using the tracks with large impact parameter. This new isolation cut will work to reject the $b\overline{b}$ rather than non-b background. Furthermore, we can search for tracks with large impact parameter on the opposite side of the dimuon candidates to make sure that the b and $\overline{b}$ go to the opposite side.

Therefore, CDF could improve the BG rejection by a factor of 200-400 with further reduction of the signal efficiency by a factor of 2-3. Based on these facts, we now consider two cases to evaluate Run II limits as a function of luminosity.

In the first case (Case A), we naively assume new tighter cuts in Run II, described above, will gain additional BG rejection power of 450 for additonal efficiency of 0.45, or $\mathcal{R}_2 = 450^{0.45/\epsilon_2}$. This gives us

$$\frac{\epsilon_2}{\epsilon_1} = \frac{1}{1 + \log(\mathcal{R}_2/\mathcal{R}_1)/\log(450)} \tag{3}$$

If we could optimize the BG rejection in Run IIa (2 fb^{-1}) to be $\mathcal{R}_2 \approx 51\mathcal{R}_1$ with $\epsilon_2 \approx 0.61\epsilon_1$ (from Eq. 3), then we would expect one BG event in 2 fb^{-1}. Thus, with an assumption of the same size of the total systematic uncertainty in Run II as in Run I, we can extrapolate the 95% C.L. limit to be $Br < 7.7 \times 10^{-8}$ for 2 fb^{-1} using $N_1^{95\%}$.

In the second case (Case B), we simply assume the Run-II background rejection could be improved (without loosing the signal efficiency) to keep the expected BG events in 2 fb^{-1} at the level of Run I (*i.e.*, 0.9 events). If we would observe one event in 2 fb^{-1}, then we could set the limits by scaling the Run-I Br limit down by the luminosity (2000 pb^{-1}/98 pb^{-1}) and the acceptance by (2.8/1.0). Thus we obtain $Br < 4.6 \times 10^{-8}$. This would certainly be the optimistic scenario, but it would be a goal of this analysis in Run IIa. Here, the systematic uncertainty in Run II is assummed to be the same as in Run I.

We repeat the same arguement for different luminosities. Figure 2 shows 95% C.L. limits on $Br[B_s \to \mu^+\mu^-]$ at CDF in Run II as a function of integrated luminosity for Cases A and B. For 15 fb^{-1} in case A, CDF would be sensitive to $Br > 1.2 \times 10^{-8}$ and the combined CDF and D0 data (30 fb^{-1}) would be sensitive to $Br > 6.5 \times 10^{-9}$.

5. RESULTS FOR MSUGRA. We examine first the parameter region for the mSUGRA model that would be accessible to CDF at Run II with 15 fb^{-1} of data. Figure 3 shows the $Br[B_s \to \mu^+\mu^-]$ as a function of $m_{1/2}$ for $A_0 = 0$, $m_0 = 300$ GeV. One sees that with a sensitivity of $Br[B_s \to \mu^+\mu^-] > 1.2 \times 10^{-8}$ for 15 fb^{-1}, the Tevatron Run II can probe the $B_s \to \mu^+\mu^-$ decay for $\tan\beta > 30$. Further, a search for this decay would sample much higher regions of $m_{1/2}$ than a direct search at Run II for SUSY particles which is restricted to $m_{1/2} < 250$ GeV [26]. As m_0 increases, the branching ratio goes down. However, this dependence becomes less significant for large $m_{1/2}$, where m_0 as large as 800 GeV can be sampled for large $m_{1/2}$.

In Figure 4 the contours of $Br[B_s \to \mu^+\mu^-]$ are plotted in the m_0-$m_{1/2}$ plane for $\tan\beta = 50$, $A_0 = 0$. We combine now this result with the other experimental constraints. Thus the shaded region to the left is ruled out by the $b \to s\gamma$ constraint, and the shaded region on the right hand side is disallowed if $a_\mu^{\rm SUGRA} > 11 \times 10^{-10}$. The narrow shaded band in the middle is allowed by the dark matter constraint. We note that independent of whether the astronomically observed dark matter is SUSY in origin, the dark matter allowed region for mSUGRA cannot significantly deviate from this shaded region, for below the narrow shaded band, the stau would be lighter than the neutralino (leading to charged dark matter), while above the band, mSUGRA would predict more neutralino dark matter than is observed.

Using our estimate that $Br > 1.2 \times 10^{-8}$ can be observed with 15 fb^{-1}, we see that almost the entire parameter space allowed by the a_μ constraint can be probed in Run II for $\tan\beta = 50$. Note that an observed $Br[B_s \to \mu^+\mu^-] > 7 \times 10^{-8}$, possible with only 2

fb^{-1}(see Figure 2), would be sufficient to rule out the mSUGRA model for $\tan\beta \leq 50$. In Figure 4 we also show the expected dark matter detector cross section for Milky Way dark matter (the short solid lines). They are of a size that can be observed by future planned dark matter detectors such as GENIUS, Cryoarray, ZEPLIN IV and CUORE. In Figure 5 we plot the same information for $\tan\beta = 40$, $A_0 = 0$. We see here about half the parameter space can be scanned by the CDF detector (and the whole parameter space if a similar analysis holds for the D0 detector). See Figure 2. We note, further, that if $A_0 = 0$, a simultaneous measurement of both $Br[B_s \to \mu^+\mu^-]$ and a_μ would essentially determine the mSUGRA parameters, as the m_0 allowed region at fixed $m_{1/2}$ is very narrow due to the dark matter constraint. The effect of varying A_0 is shown in Figure 6, where the allowed region for $A_0 = -2m_{1/2}$, $\tan\beta = 40$ in the m_0-$m_{1/2}$ plane is plotted. The effect is to tilt (and narrow) the allowed dark matter band. The entire allowed parameter space can again be probed.

In Figures 4, 5 and 6, we have also drawn lines for various light Higgs masses (vertical dotted lines). A measurement of $B_s \to \mu^+\mu^-$, a_μ and m_h would then effectively determine the parameters of mSUGRA for $\mu > 0$ by requiring that they intersect with the dark matter allowed band at a point. (If no choice of parameters allowed this, mSUGRA would be ruled out.) The Tevatron Run II should be able to either rule out a Higgs mass or give evidence for its existence at the 3 σ level over the entire allowed mass range of SUSY light Higgs masses. Alternatively, the LHC's determination of m_h or the gluino mass (to determine $m_{1/2}$) would fix the parameters of mSUGRA.

The BNL E821 experiment should shortly have a more accurate value for a_μ, with errors reduced by a factor of two or more. We note from the above figures the importance this result might have. Thus if a_μ increases, the a_μ bound moves downward, encroaching further on the allowed part of the parameter space, and a value of $a_\mu \gtrsim 50 \times 10^{-10}$ would eliminate the mSUGRA model [27]. However, if a_μ decreases significantly (but is still positive), the mSUGRA model would predict a heavy SUSY particle spectra closer to the TeV region, having significant effects on accelerator and dark matter detection physics. An accurate determination of a_μ corresponds to a line from upper left to lower right (or more precisely a band when errors are included) running parallel to the $a_\mu < 11 \times 10^{-10}$ boundary, and cutting through the allowed dark matter band which runs from lower left to upper right. Thus these two experiments are complementary for determining the mSUGRA parameters.

6. R PARITY VIOLATING MODELS. We consider briefly here the case when R parity is broken. The general renormalizable R parity violating superpotential has the form

$$W_{\not R_p} = \kappa_i L_i H_2 + \lambda_{ijk} L_i L_j E^c_k + \lambda'_{ijk} L_i Q_j D^c_k + \lambda''_{ijk} U^c_i D^c_j D^c_k \tag{4}$$

The first three terms are lepton number violating, and the last term is baryon number violating. For the $B_s \to \mu^+\mu^-$ decay, we need to consider lepton violating terms [28], and so we set λ'' to zero (to prevent rapid proton decay). Unlike the R parity conserving models, the SUSY contribution to $B_s \to \mu^+\mu^-$ can now occur at the tree level, and so can be considerably larger. For example, if the λ and λ' terms are present in the theory, we can have

$$C_S = -\frac{\lambda'_{i23}\lambda^*_{i22}}{2m^2_{\tilde\nu}},\ C_P = \frac{\lambda'_{i23}\lambda^*_{i22}}{2m^2_{\tilde\nu}}. \tag{5}$$

In Figure 7, we plot the Br as a function of $m_{1/2}$ in the R parity violating scenarios. We have chosen $\lambda'_{i23} = \lambda_{i22} = 0.02$ and $\tan\beta = 10$. These small couplings are not restricted by

any another physical process [29]. We see that in this case smaller values of $\tan\beta$ can be probed and the Br is large compared to the R parity conserving case. The contributions of $C_{S,P}$ to the newly discovered decay mode $B_s \to K\mu\mu$ are small. For example, for $m_{1/2} =$ 300 GeV and $m_0 = 300$ GeV, $Br[B_s \to K\mu\mu]$ gets a contribution of 3.30×10^{-7}. (This calculation, however, involves a large QCD uncertainty.) The observed branching fraction for this mode is $(0.99^{+0.4+0.13}_{-0.3-0.14}) \times 10^{-6}$ [30].

In contrast to the R conserving case, the R parity violating scenarios are not infested with tau's and therefore has the potential to be observed at Run II directly. For example, let us consider the production of $\chi_1^{\pm}\chi_2^0$ and let us assume that λ_{i22}, λ'_{i23} are present. In this case we can have several interesting final states such as $6l$ + 2jets+missing E_T (from neutrino) and $4l$ + 4jet+missing E_T from the production of $\tilde{\chi}_1^{\pm}$-$\tilde{\chi}_2^0$.

7. CONCLUSIONS. We have investigated the prospects for studying the rare decay mode $B_s \to \mu^+\mu^-$ by the CDF detector in Run II at the Tevatron. We have analyzed the background for this process and find that a $Br > 1.2\times10^{-8}$ for 15 fb^{-1} can be probed at Run II. (This is nearly a factor of 100 improvement over the Run I bound.) In this background analysis, we have not only extrapolated the Run I limit, but also introduced new selection cuts to reduce the background. The improvement of the Run II detector has also been taken into account. If a similar analysis can be performed for the D0 detector, the combined data would increase the sensitivity for detecting this decay mode to $Br > 6.5 \times 10^{-9}$. The LHC should be able to reach the sensitivity at the level of SM branching ratio [31].

The $B_s \to \mu^+\mu^-$ is an important process for SUSY searches for new physics, as the Standard Model prediction of the branching ratio is quite small (3.5×10^{-9}), and the SUSY contribution increases for large $\tan\beta$ as $\tan^6\beta$. For the mSUGRA model, the above sensitivity implies that Run II could probe a region of parameter space for $\tan\beta > 30$, a region which could not be probed by a direct search at Run II. We have combined the expectations for $B_s \to \mu^+\mu^-$ for mSUGRA with other experimental bounds on the parameter space. Thus a large branching ratio, *i.e.*, $> 7 \times 10^{-8}(14 \times 10^{-8})$ would be sufficient to eliminate the mSUGRA model for $\tan\beta \leq 50(55)$. A measurement of $B_s \to \mu^+\mu^-$, the muon $g-2$ anomaly and the light Higgs mass combined with the astronomical bounds on cold dark matter would essentially determine the mSUGRA model, allowing predictions of all other sparticle masses and cold dark matter neutralino-proton cross sections. If the muon $g-2$ anomaly remains positive these cross sections are $\gtrsim 10^{-9}$ pb, and should then be accessible to future planned detectors such as GENIUS, Cryoarray, ZEPLIN IV and CUORE.

A simple model of R parity violation was also considered, and here the $Br[B_s \to \mu^+\mu^-]$ can be large for both small and large $\tan\beta$.

ACKNOWLEDGEMENTS This work was supported in part by National Science Foundation grant PHY-0101015 and in part by Department of Energy grant DE-FG03-95ER40917. We should like to thank D. Toback for valuable comments.

REFERENCES

[1] P. Langacker, in *Proc. of the APS/DPF/DPB Summer Study on the Future of Particle Physics (Snowmass 2001)* ed. R. Davidson and C. Quigg, arXiv:hep-ph/0110129.

[2] K. Anikeev *et al.*, arXiv:hep-ph/0201071.

[3] K. S. Babu and C. Kolda, Phys. Rev. Lett. **84**, (2000) 228.

[4] P. H. Chankowski and L. Slawianowska, Acta Phys. Polon. B **32**, (2001) 1895.

[5] C. Bobeth, T. Ewerth, F. Kruger and J. Urban, Phys. Rev. D **64**, (2001) 074014.

[6] A. Dedes, H. K. Dreiner and U. Nierste, Phys. Rev. Lett. **87**, (2001) 251804.

[7] G. Isidori and A. Retico, JHEP **0111**, (2001) 001.

[8] C. S. Huang and W. Liao, Phys. Rev. D **63** (2001) 11402; (E) D**64** (2001) 059902; arXiv:hep-ph/0201121.

[9] A. H. Chamseddine, R. Arnowitt and P. Nath, Phys. Rev. Lett. **49**, (1982) 970.

[10] R. Barbieri, S. Ferrara and C. A. Savoy, Phys. Lett. B **119**, (1982) 343;L. J. Hall, J. Lykken and S. Weinberg, Phys. Rev. D **27** (1983) 2359; P. Nath, R. Arnowitt and A. H. Chamseddine, Nucl. Phys. B **227**, (1983) 121.

[11] CLEO Collaboration, S. Chen *et al.*, Phys. Rev. Lett. **87**, (2001) 251807.

[12] P. Igo-Kemenes, LEPC meeting, November 3, 2000 (http://lephiggs.web.cern.ch/LEPHIGGS/talks/index.html).

[13] R. Rattazzi and U. Sarid, Phys. Rev. D **53**, (1996) 1553; M. Carena, M. Olechowski, S. Pokorski and C. E. Wagner, Nucl. Phys. B **426**, (1994) 269.

[14] T. C. Yuan, R. Arnowitt, A. H. Chamseddine and P. Nath, Z. Phys. C **26**, (1984) 407.

[15] D. A. Kosower, L. M. Krauss and N. Sakai, Phys. Lett. B **133**, (1983) 305.

[16] M. Knecht, A. Nyffeler, M. Perrottet and E. De Rafael, Phys. Rev. Lett. **88**, (2002) 071802.

[17] M. Hayakawa and T. Kinoshita, arXiv:hep-ph/0112102.

[18] M. S. Turner, arXiv:astro-ph/0202007.

[19] R. Arnowitt, B. Dutta and Y. Santoso, Nucl. Phys. B **606**, (2001) 59.

[20] J. R. Ellis, T. Falk, G. Ganis, K. A. Olive and M. Srednicki, Phys. Lett. B **510**, (2001) 236; J. R. Ellis, T. Falk and K. A. Olive, Phys. Lett. B **444**, (1998) 367; J. R. Ellis, T. Falk, K. A. Olive and M. Srednicki, Astropart. Phys. **13**, (2000) 181 [Erratum-ibid. **15**, (2000) 413].

[21] M. E. Gomez, G. K. Leontaris, S. Lola and J. D. Vergados, Phys. Rev. D **59**, (1999) 116009; M. Gomez, G. Lazarides, C. Pallis, Phys. Rev. D **61**, (2000) 123512; Phys. Lett. B **487**, (2000) 313.

[22] M. Carena, D. Garcia, U. Nierste and C. E. Wagner, Nucl. Phys. B **577**, (2000) 88.

[23] CDF Collaboration, F. Abe *et al.*, Phys. Rev. D **57**, (1998) 3811.

[24] We use a coordinate system where θ and ϕ are the polar and azimuthal angles, respectively, with respect to the proton beam direction (z axis). The pseudorapidity (η) is defined as $-ln[\tan(\theta/2)]$. The transverse momentum of a particle is denoted as $p_T = p\, sin\theta$.

[25] CDF Collaboration, T. Affolder *et al.*, Phys. Rev. Lett. **83**, (1999) 3378.

[26] V. D. Barger and C. Kao, Phys. Rev. D **60**, (1999) 115015.

[27] R. Arnowitt, B. Dutta, B. Hu and Y. Santoso, Phys. Lett. B **505**, (2001) 177.

[28] J-H. Jang, J. K. Kim and J. S. Lee Phys. Rev. D**55**, (1997) 7296.

[29] G. Bhattacharyya, arXiv:hep-ph/9709395; B. C. Allanach, A. Dedes and H. K. Dreiner, Phys. Rev. D **60**, (1999) 075014.

[30] BELLE Collaboration, K. Abe *et al.*, Phys. Rev. Lett. **88**, (2002) 021801.
[31] A. Nikitenko, A. Starodumov and N. Stepanov, arXiv:hep-ph/9907256.

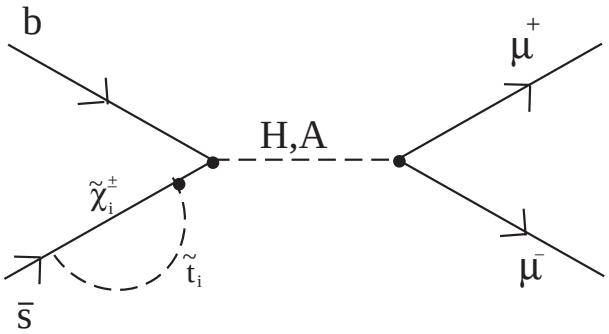

FIG. 1. Example of diagram contributing to $B_s \to \mu^+\mu^-$ with leading contribution of $\tan^3\beta$. The H and A are the heavy CP even and CP odd neutral Higgs bosons, $\tilde{\chi}_i^{\pm}$ $(i = 1, 2)$ are charginos and $\tilde{t}_i (i = 1, 2)$ are the stop bosons. Heavy marked vertices each contain a factor of $\tan\beta$.

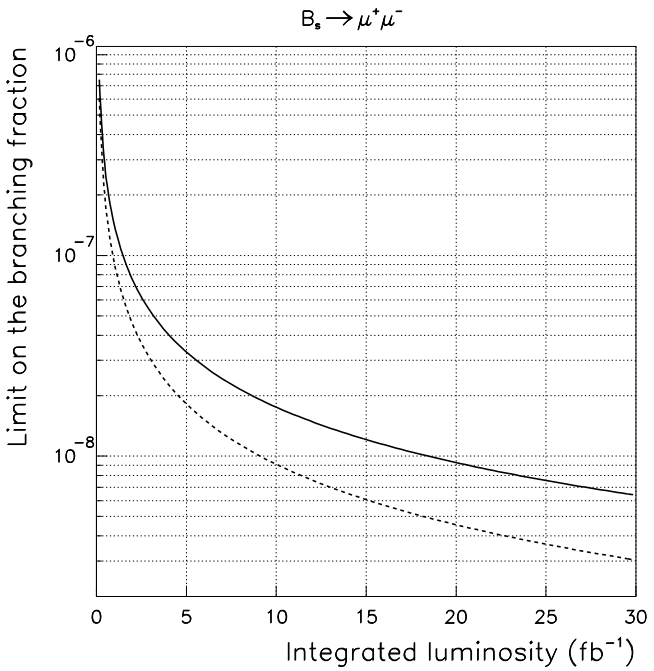

FIG. 2. Illustrated 95% C.L. limits on the branching ratio for $B_s \to \mu^+\mu^-$ at CDF in Run II as a function of integrated luminosity. Solid (Case A) and dashed (Case B) curves are based on different assumptions on the signal selection efficiency and the background rejection power. See the text for details.

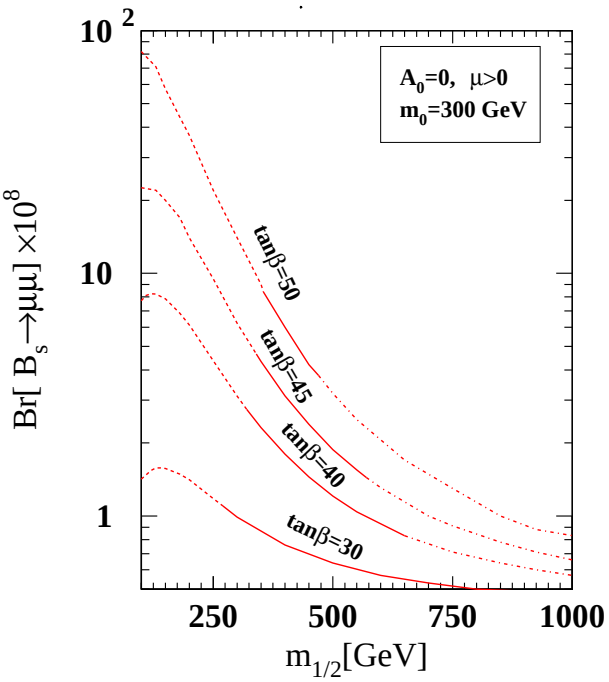

FIG. 3. Branching ratio for $B_s \to \mu^+\mu^-$ as a function of $m_{1/2}$ for various $\tan\beta$ values in mSUGRA models. Other mSUGRA parameters are fixed to be $m_0 = 300$ GeV, $A_0 = 0$ and $\mu > 0$. Dashed and dash-dotted lines are to indicate the models are excluded via constraints on $Br[b \to s\gamma]$ and $m_{\tilde{\tau}} > m_{\tilde{\chi}_1^0}$, respectively.

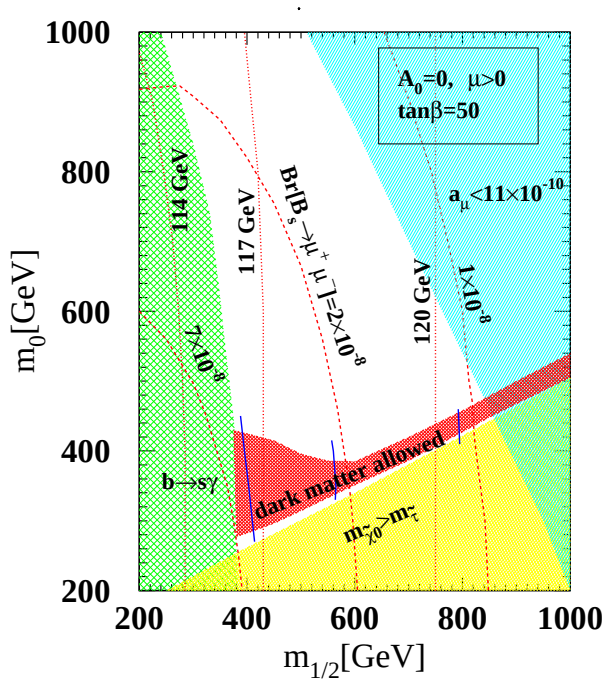

FIG. 4. Branching ratio for $B_s \to \mu^+\mu^-$ (three dashed lines from left to right: 7×10^{-8}, 2×10^{-8}, 1×10^{-8}) for $\tan\beta = 50$ in the m_0-$m_{1/2}$ plane. Other mSUGRA parameters are fixed to be $A_0 = 0$ and $\mu > 0$. The three short solid lines indicate the $\sigma_{\tilde{\chi}_1^0 - p}$ values (from left: 0.05 $\times 10^{-6}$ pb, 0.004 $\times 10^{-6}$ pb, 0.002 $\times 10^{-6}$ pb). The vertical dotted lines label Higgs masses.

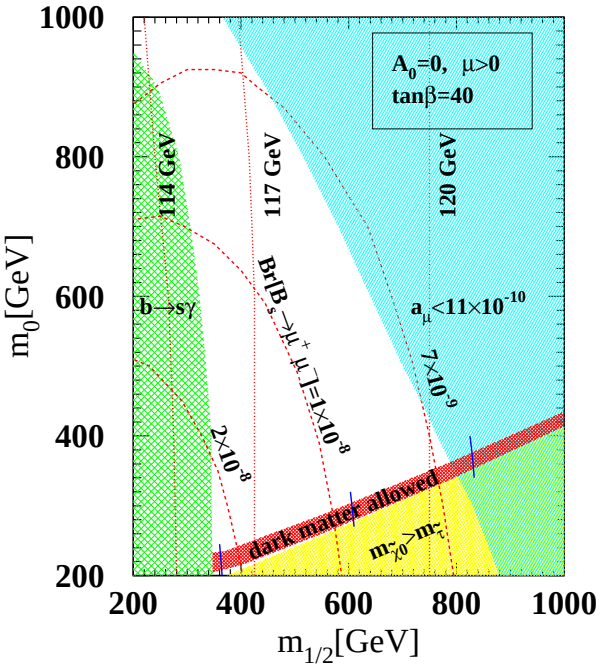

FIG. 5. Branching ratio for $B_s \to \mu^+\mu^-$ (three dashed lines from left to right: 1.9×10^{-8}, 1×10^{-8}, 0.7×10^{-8}) at $\tan\beta = 40$ in the m_0-$m_{1/2}$ plane. Other mSUGRA parameters are fixed to be $A_0 = 0$ and $\mu > 0$. The three short solid lines indicate the $\sigma_{\tilde{\chi}_1^0 - p}$ values (from left: 0.03 $\times 10^{-6}$ pb, 0.002 $\times 10^{-6}$ pb, 0.001 $\times 10^{-6}$ pb). The vertical dotted lines label Higgs masses.

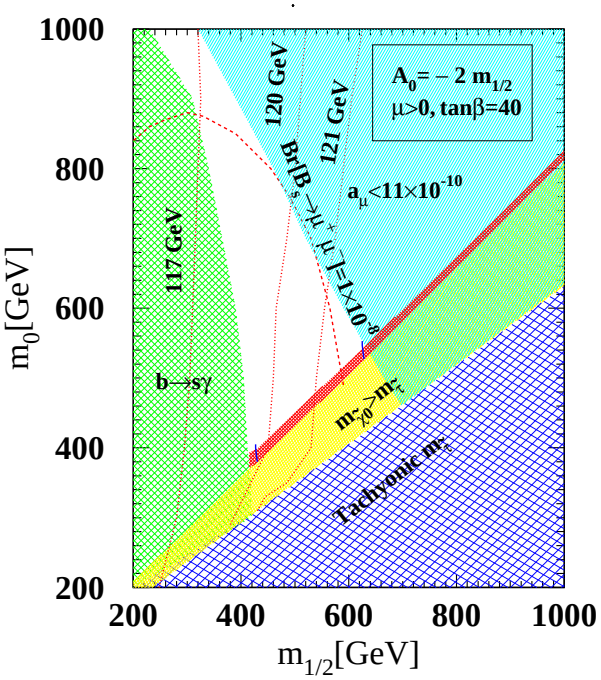

FIG. 6. Branching ratio for $B_s \to \mu^+\mu^-$ at $\tan\beta = 40$ in the m_0-$m_{1/2}$ plane for $A_0 = -2m_{1/2}$ and $\mu > 0$. The two short solid lines indicate the $\sigma_{\tilde{\chi}_1^0 - p}$ values (from left: 0.005×10^{-6} pb, 0.001 $\times 10^{-6}$ pb). The vertical dotted lines label Higgs masses.

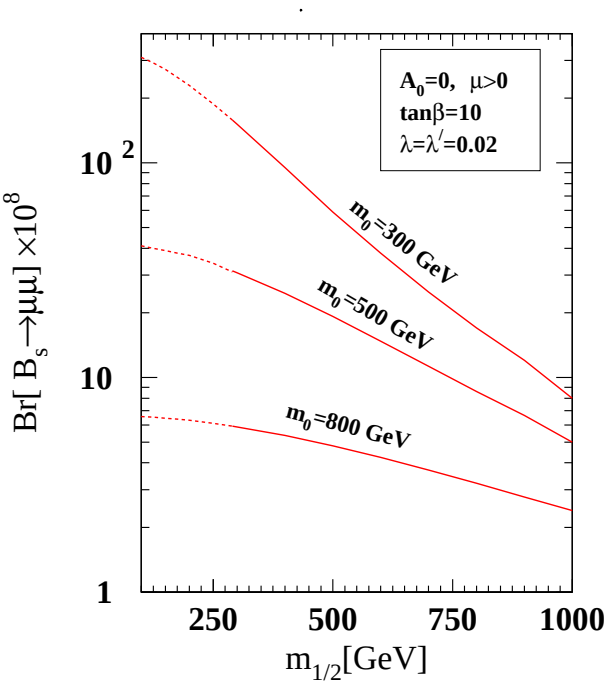

FIG. 7. Branching ratio for $B_s \to \mu^+\mu^-$ as a function of $m_{1/2}$ (in GeV) for $m_0 = 300$, 500, and 800 GeVin a $\not{R}_p$ SUSY scenario ($\lambda_{i22} = \lambda'_{i32} = 0.02$). Other mSUGRA parameters are fixed to be $\tan\beta = 10$, $A_0 = 0$ and $\mu > 0$. Dashed lines are to indicate the models that are excluded via the $b \to s\gamma$ constraints.